Hindawi Publishing Corporation
Advances in High Energy Physics
Volume 2016, Article ID 9632126, 10 pages
http://dx.doi.org/10.1155/2016/9632126

Research Article

Comparing the Tsallis Distribution with and without Thermodynamical Description in $p + p$ Collisions

H. Zheng[1] and Lilin Zhu[2]

[1]*Laboratori Nazionali del Sud, INFN, Via Santa Sofia 62, 95123 Catania, Italy*
[2]*College of Physical Science and Technology, Sichuan University, Chengdu 610064, China*

Correspondence should be addressed to Lilin Zhu; zhulilin@scu.edu.cn

Received 8 December 2015; Revised 11 March 2016; Accepted 24 March 2016

Academic Editor: Adrian Buzatu

We compare two types of Tsallis distribution, that is, with and without thermodynamical description, using the experimental data from the STAR, PHENIX, ALICE, and CMS Collaborations on the rapidity and energy dependence of the transverse momentum spectra in $p+p$ collisions. Both of them can fit the particle spectra well. We show that the Tsallis distribution with thermodynamical description gives lower temperatures than the ones without it. The extra factor m_T (transverse mass) in the Tsallis distribution with thermodynamical description plays an important role in the discrepancies between the two types of Tsallis distribution. But for the heavy particles, the choice to use m_T or E_T (transverse energy) in the Tsallis distribution becomes more crucial.

1. Introduction

The particle spectrum is a basic quantity directly measured in the experiments and it can reveal the information of particle production mechanism in heavy-ion collisions. Many physicists have devoted themselves to studying the particle spectra produced in the heavy-ion collisions using thermodynamical approaches, phenomenological methods, transport models, and so forth [1–22]. Recently, the Tsallis distribution, which was first proposed about twenty-seven years ago as a generalization of the Boltzmann-Gibbs distribution [23], has attracted many theorists' and experimentalists' attention in high energy collisions [5–9, 11–17, 24–34]. The excellent ability to fit the spectra of identified hadrons and charged particles in a large range of p_T up to 200 GeV/c, which covers 15 orders of magnitude, is quite impressive. This spectacular result was first shown by Wong et al. [14–16]. In [21, 22], we have shown that Tsallis distribution can fit almost all the particle spectra produced in $p + p$, $p + A$, and $A + A$ at RHIC and LHC. From the phenomenological view, there may be real physics behind the prominently phenomenological work, for example, Regge trajectory for particle classification [35]. We also note that there are different versions of Tsallis distribution in the literature and we classify them as Type A, Type B, and Type C to clarify the comparison in [21]. Type A Tsallis distribution is obtained without resorting to thermodynamical description, but it has been adopted to analyze the particle spectra by STAR [24] and PHENIX [25] Collaborations at RHIC and ALICE [26–28] and CMS [29] Collaborations at LHC. In [21], we applied it to do the systematic analysis of identified particle spectra in $p + p$ collisions at RHIC and LHC and proposed a cascade particle production mechanism. On the other hand, Type B Tsallis distribution is derived by taking into account the thermodynamical consistency and is widely used by Cleymans and his collaborators to study the particle spectra in high energy $p+p$ collisions [8–10]. It is also used by other authors for nucleus-nucleus interactions [11]. Type A and Type B are the most popular Tsallis distributions in the literature but they give quite different temperatures while fitting the same particle spectra; for example, for pion, Type A gives $T \sim 0.13$ GeV while Type B gives $T \sim 0.075$ GeV. In this paper, we would like to systematically address the question regarding the discrepancies of the temperatures for the two types of Tsallis distribution, by using particle spectra in $p + p$ collisions. The data produced in $p + p$ collisions with different p_T ranges and different rapidity cuts are collected from the experimental collaborations at RHIC and LHC [25–27, 30, 36–42].

The paper is organized as follows. In Section 2, we introduce the two types of Tsallis distribution, without and with thermodynamical description, in our comparison. In order to make our discussion clear, we also introduce another three transient distributions which are very similar to Type A and Type B Tsallis distributions. In Section 3, the results of particle spectra from the different distributions in $p + p$ collisions and the comparisons are shown. A brief conclusion is given in Section 4.

2. Tsallis Distributions

Type A Tsallis distribution has been widely adopted by STAR [24] and PHENIX [25] Collaborations at RHIC and ALICE [26–28] and CMS [29] Collaborations at LHC:

$$E\frac{d^3N}{dp^3} = \frac{dN}{dy}\frac{(n-1)(n-2)}{2\pi nC\left[nC + m(n-2)\right]}\left(1 + \frac{m_T - m}{nC}\right)^{-n}, \quad (1)$$

where $m_T = \sqrt{p_T^2 + m^2}$ is the transverse mass, dN/dy, n, and C are fitting parameters, and m was used as a fitting parameter in [24], but it represents the rest mass of the particle studied in [25–29]. When $p_T \gg m$, we can ignore m in the last term in (1) and obtain $E(d^3N/dp^3) \propto p_T^{-n}$. This result is well known because high energy particles come from hard scattering and they follow a power law distribution with p_T. When $p_T \ll m$ which is the nonrelativistic limit, we obtain $m_T - m = p_T^2/2m = E_T^{\text{classical}}$ and $E(d^3N/dp^3) \propto e^{-E_T^{\text{classical}}/C}$, that is, a thermal distribution. The parameter C in (1) plays the same role as temperature T. In [21, 22], we have obtained the simpler form of (1):

$$\left(E\frac{d^3N}{dp^3}\right)_{|\eta|<a} = A\left(1 + \frac{E_T}{nT}\right)^{-n}, \quad (2)$$

where the transverse energy $E_T = m_T - m$. A, n, and T are free fitting parameters in (2). We note that it has been used by CMS Collaboration [31, 32, 43] and by Wong et al. in their recent paper [16]. The STAR Collaboration also applied a formula which is very close to (2) [44]. We adopt (2) in the following study.

In the framework of Tsallis statistics, the distribution function is

$$f(E,q) = \left[1 + (q-1)\frac{E-\mu}{T}\right]^{-1/(q-1)}. \quad (3)$$

Taking into account the self-consistent thermodynamical description, one has to use the effective distribution $[f(E,q)]^q$. Therefore, the Tsallis distribution is obtained [8, 9, 11, 12]:

$$E\frac{d^3N}{dp^3} = gV\frac{m_T\cosh y}{(2\pi)^3}\left[1 + (q-1)\frac{m_T\cosh y - \mu}{T}\right]^{-q/(q-1)}, \quad (4)$$

where g is the degeneracy of the particle state, V is the volume, y is the rapidity, μ is the chemical potential, T is the temperature, and q is the entropic factor, which measures the nonadditivity of the entropy. We dubbed it as the Type B Tsallis distribution [21]. In (4), there are four parameters, namely, V, μ, T, and q. μ was assumed to be 0 in [8, 9, 11] which is a reasonable assumption because the energy is high enough and the chemical potential is much smaller than the temperature. In the midrapidity $y = 0$ region, (4) is reduced to

$$E\frac{d^3N}{dp^3} = gV\frac{m_T}{(2\pi)^3}\left[1 + (q-1)\frac{m_T}{T}\right]^{-q/(q-1)}. \quad (5)$$

It becomes very similar to (2), but there are some differences; for example, m_T replaces E_T in the bracket and there is an extra term m_T in front of the bracket. It should be pointed out that there is no direct match between n and q in (2) and (5). But we could find a connection between n and q in the limit at large p_T. When $p_T \gg m$, from (5), we can obtain

$$E\frac{d^3N}{dp^3} \propto p_T^{-1/(q-1)}. \quad (6)$$

Recalling that $E(d^3N/dp^3) \propto p_T^{-n}$ when $p_T \gg m$ from (1), the relation between n and q is

$$n = \frac{1}{q-1}. \quad (7)$$

Another treatment to find the relation between n and q can be found in [10].

For the other Tsallis distributions in the literature, we refer them to [21, 22]. We noted that Type A and Type B Tsallis distributions can reproduce the particle spectra in $p+p$ collisions very well, but Type B gives lower temperatures than the ones given by Type A. In this paper, we would like to address this discrepancies between the two types of Tsallis distribution. To make our discussion clear, another three transient distributions are used to bridge Type A and Type B distributions. In [45], a Tsallis-like distribution is obtained in the framework of nonextensive statistics for the particle invariant yield at midrapidity:

$$E\frac{d^3N}{dp^3} = Am_T\left[1 + (q-1)\frac{m_T}{T}\right]^{-1/(q-1)}, \quad (8)$$

where A, q, and T are fitting parameters. Comparing (8) and (5), the only difference is the power of the distribution function, that is, q for (5) and 1 for (8). We also introduce another two forms of distribution. One is

$$E\frac{d^3N}{dp^3} = A\left[1 + (q-1)\frac{m_T}{T}\right]^{-q/(q-1)}, \quad (9)$$

where we neglect the term m_T outside of the bracket in (5) and the constants are absorbed into the parameter A. The other one is

$$E\frac{d^3N}{dp^3} = A\left[1 + (q-1)\frac{m_T}{T}\right]^{-1/(q-1)}. \quad (10)$$

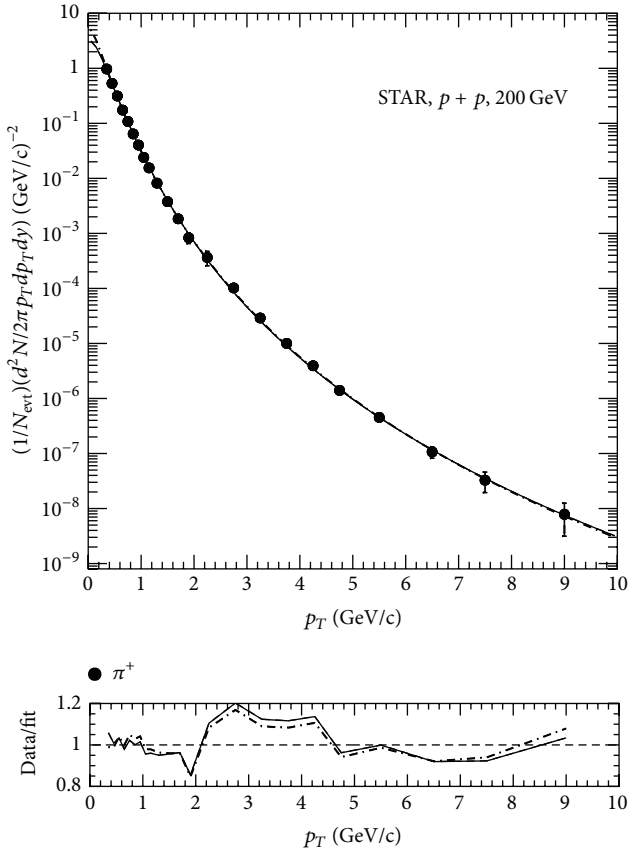

FIGURE 1: Fitting results using the distributions equations (5), (8), (9), (10), and (2) for π^+ in $p + p$ collisions at $\sqrt{s} = 200$ GeV. The solid line, dashed line, dotted line, dash-dotted line, and bold dash-dotted line refer to (5), (8), (9), (10), and (2), respectively, but they are hardly to distinguish. The ratios of data/fit are shown at the bottom. Data are taken from STAR [39].

Similar to (9), we neglect the term m_T in front of the bracket in (8) but keep the rest. Using the relation equation (7), we find that (10) becomes (2) in the limit of massless particle.

Let us put the four distributions in order of (5), (8), (10), and (2) and (5), (9), (10), and (2); one can see that any adjacent distributions have only one term different. We successfully bridge Type A and Type B Tsallis distributions and are able to conduct our investigation. We need to point out that even though we use the same symbols for the parameters in all five distributions, they may have different values when fitting the experimental data. In the next section, we will systematically apply the five distributions to the particle spectra in $p + p$ collisions, similar to our previous work [21]. But we update some experimental data which have larger p_T ranges and will focus on the temperature differences among the five distributions.

3. Results

We fit the particle spectra with different p_T ranges and different rapidity cuts from $p + p$ collisions at $\sqrt{s} = 62.4$, 200, 900, 2760, and 7000 GeV with the five distributions discussed in the last section. The fitting process is the same as that in [21, 22]. Compared with [21], the identified particle spectra data at $\sqrt{s} = 2760$ and 7000 GeV have been updated.

In this work, we are interested in the differences of the parameter T from the five distributions. As we argued in [21, 22], T is one free fitting parameter and can be different for different particles even though they are produced in the same colliding system. In order to distinguish the parameters T and q in the distributions and make our discussion clear, we assign $T_1(q_1)$, $T_2(q_2)$, $T_3(q_3)$, and $T_4(q_4)$ to (5), (8), (9), and (10), respectively, while we assign T_5 and n for (2). All the five distributions can fit the particle transverse momentum spectra very well. The values of T_i ($i = 1, 2, 3, 4, 5$), q_i ($i = 1, 2, 3, 4$), n, and corresponding χ_i^2/ndf for π, K, p, and charged particles are shown in Tables 1 and 2. Furthermore, the errors of T_i, q_i and n are also provided in the tables. Here, we only show the fitting results with the five distributions for four cases: (1) π^+ at $\sqrt{s} = 200$ GeV, (2) π^+ at $\sqrt{s} = 900$ GeV, (3) $K^+ + K^-$ at $\sqrt{s} = 2760$ GeV, and (4) $p + \overline{p}$ at $\sqrt{s} = 7000$ GeV.

In Figures 1 and 2, we show the fitting results for π^+ at $\sqrt{s} = 200$ GeV from STAR Collaboration and $\sqrt{s} = 900$ GeV

Table 1: The fitting parameters T_i, q_i ($i = 1, 2, 3$), the errors of parameters, and χ^2/ndf in (5), (8), and (9) for the particle spectra in $p + p$ collisions. The unit of T is GeV.

Data source	$\sqrt{s}$ (GeV)	Particle	T_1	q_1	χ_1^2/ndf	T_2	q_2	χ_2^2/ndf	T_3	q_3	χ_3^2/ndf
PHENIX [37]	62.4	π^0	0.106 ± 0.001	1.076 ± 0.0009	2.923/11	0.101 ± 0.0001	1.070 ± 0.0001	3.622/11	0.140 ± 0.0003	1.078 ± 0.0001	1.353/11
PHENIX [25]	62.4	π^+	0.0905 ± 0.0001	1.092 ± 0.0002	6.981/23	0.083 ± 0.0007	1.084 ± 0.0006	6.781/23	0.130 ± 0.0006	1.091 ± 0.002	4.794/23
		π^-	0.0895 ± 0.0004	1.091 ± 0.0009	8.617/23	0.0824 ± 0.001	1.083 ± 0.002	8.805/23	0.125 ± 0.0001	1.093 ± 0.0001	5.383/23
		K^+	0.0979 ± 0.0005	1.097 ± 0.002	5.205/13	0.0767 ± 0.0004	1.100 ± 0.0008	5.253/13	0.130 ± 0.0005	1.110 ± 0.001	5.346/13
		K^-	0.0959 ± 0.0002	1.093 ± 0.0001	2.718/13	0.0773 ± 0.0005	1.093 ± 0.001	2.432/13	0.132 ± 0.001	1.096 ± 0.004	2.285/13
		p	0.100 ± 0.0001	1.065 ± 0.0002	6.755/24	0.088 ± 0.0001	1.063 ± 0.0001	6.855/24	0.108 ± 0.0001	1.075 ± 0.0002	7.651/24
		$\overline{p}$	0.0894 ± 0.0001	1.064 ± 0.0002	3.655/22	0.0901 ± 0.0001	1.057 ± 0.0001	3.637/22	0.0906 ± 0.0001	1.079 ± 0.0002	5.931/22
PHENIX [38]	200	π^0	0.0898 ± 0.0005	1.107 ± 0.0006	17.137/22	0.0787 ± 0.0004	1.098 ± 0.0004	20.184/22	0.114 ± 0.0003	1.121 ± 0.0002	27.743/22
PHENIX [25]	200	π^+	0.0747 ± 0.0001	1.126 ± 0.0005	5.638/24	0.0671 ± 0.0001	1.112 ± 0.0002	5.816/24	0.111 ± 0.0001	1.138 ± 0.0006	4.698/24
		π^-	0.0799 ± 0.0001	1.121 ± 0.0001	4.861/24	0.0718 ± 0.0001	1.107 ± 0.0003	4.652/24	0.121 ± 0.0001	1.126 ± 0.0002	3.547/24
		K^+	0.0416 ± 0.0001	1.166 ± 0.0005	1.886/13	0.0494 ± 0.0004	1.131 ± 0.002	2.157/13	0.0819 ± 0.0001	1.176 ± 0.003	2.062/13
		K^-	0.0672 ± 0.0001	1.140 ± 0.0003	3.819/13	0.0613 ± 0.0001	1.121 ± 0.0003	4.039/13	0.0960 ± 0.0001	1.162 ± 0.0004	3.355/13
		p	0.0444 ± 0.0001	1.111 ± 0.0002	19.868/31	0.0395 ± 0.0001	1.100 ± 0.0001	19.986/31	0.0386 ± 0.0001	1.135 ± 0.0001	24.485/31
		$\overline{p}$	0.0414 ± 0.0001	1.110 ± 0.0001	15.918/31	0.0321 ± 0.001	1.102 ± 0.005	20.450/31	0.0541 ± 0.0001	1.122 ± 0.0002	15.892/31
STAR [39]	200	π^+	0.0860 ± 0.0001	1.108 ± 0.0003	6.953/20	0.0735 ± 0.0001	1.099 ± 0.0002	12.536/20	0.124 ± 0.0001	1.115 ± 0.0002	5.979/20
		π^-	0.0884 ± 0.0003	1.107 ± 0.0003	6.240/20	0.0791 ± 0.003	1.097 ± 0.001	5.977/20	0.128 ± 0.0005	1.113 ± 0.0002	5.099/20
		p	0.0774 ± 0.0006	1.093 ± 0.0006	12.112/17	0.0576 ± 0.0002	1.091 ± 0.0001	11.137/17	0.074 ± 0.0001	1.115 ± 0.0002	12.495/17
		$\overline{p}$	0.0676 ± 0.0001	1.098 ± 0.0002	9.595/17	0.0620 ± 0.0001	1.090 ± 0.0001	9.017/17	0.0829 ± 0.002	1.110 ± 0.004	9.572/17
ALICE [26]	900	π^0	0.0915 ± 0.0001	1.131 ± 0.0002	7.588/10	0.0951 ± 0.0006	1.108 ± 0.0008	9.523/10	0.122 ± 0.0002	1.154 ± 0.0001	7.715/10
ALICE [27]	900	π^+	0.0712 ± 0.0002	1.147 ± 0.0006	21.599/30	0.0623 ± 0.0004	1.128 ± 0.002	21.912/30	0.123 ± 0.0002	1.148 ± 0.0005	13.382/30
		π^-	0.0723 ± 0.0002	1.144 ± 0.0001	15.642/30	0.0636 ± 0.0001	1.126 ± 0.0001	14.984/30	0.126 ± 0.0002	1.141 ± 0.003	11.206/30
		K^+	0.0656 ± 0.0001	1.168 ± 0.0008	19.692/24	0.0516 ± 0.0001	1.148 ± 0.0002	16.661/24	0.0661 ± 0.0001	1.240 ± 0.0005	16.831/24
		K^-	0.0696 ± 0.0005	1.157 ± 0.0001	7.919/24	0.0578 ± 0.0009	1.138 ± 0.002	7.240/24	0.0985 ± 0.0003	1.191 ± 0.0001	6.804/24
		p	0.0513 ± 0.0001	1.133 ± 0.0002	14.723/21	0.0466 ± 0.0001	1.117 ± 0.0002	14.808/21	0.0359 ± 0.0001	1.179 ± 0.0009	14.901/21
		$\overline{p}$	0.0446 ± 0.0001	1.137 ± 0.0006	14.094/21	0.0457 ± 0.0003	1.115 ± 0.0007	14.348/21	0.0416 ± 0.0001	1.178 ± 0.0003	16.739/21
ALICE [41]	2760	π^0	0.0945 ± 0.0001	1.141 ± 0.0002	6.164/15	0.0826 ± 0.0001	1.123 ± 0.0002	6.162/15	0.143 ± 0.0004	1.159 ± 0.0004	5.981/15
ALICE [36]	2760	$\pi^+ + \pi^-$	0.0846 ± 0.0002	1.144 ± 0.0001	167.103/60	0.0743 ± 0.0001	1.126 ± 0.0002	172.168/60	0.128 ± 0.0005	1.166 ± 0.0002	31.492/60
		$K^+ + K^-$	0.0966 ± 0.0002	1.143 ± 0.0003	10.339/55	0.0845 ± 0.0005	1.125 ± 0.0008	10.347/55	0.144 ± 0.0001	1.163 ± 0.0001	13.534/55
		$p + \overline{p}$	0.0812 ± 0.0001	1.122 ± 0.0001	27.683/46	0.0789 ± 0.001	1.106 ± 0.0007	20.581/46	0.120 ± 0.002	1.133 ± 0.0009	20.062/46
ALICE [26]	7000	π^0	0.0951 ± 0.0002	1.146 ± 0.0002	11.071/30	0.0828 ± 0.0002	1.128 ± 0.0002	11.112/30	0.139 ± 0.0001	1.170 ± 0.0002	13.443/30
ALICE [42]	7000	$\pi^+ + \pi^-$	0.0712 ± 0.0005	1.172 ± 0.0007	68.408/38	0.0608 ± 0.0005	1.147 ± 0.001	68.193/38	0.125 ± 0.0002	1.191 ± 0.0004	26.041/38
		$K^+ + K^-$	0.0986 ± 0.0001	1.158 ± 0.0008	7.807/45	0.0840 ± 0.0002	1.137 ± 0.0001	7.910/45	0.152 ± 0.0003	1.184 ± 0.0004	5.335/45
		$p + \overline{p}$	0.113 ± 0.0001	1.117 ± 0.0003	16.534/43	0.105 ± 0.0002	1.103 ± 0.0002	18.608/43	0.159 ± 0.0001	1.129 ± 0.002	13.778/43
CMS [30]	900	Charged	0.0875 ± 0.0002	1.132 ± 0.0002	63.863/17	0.0780 ± 0.0001	1.117 ± 0.0001	63.940/17	0.127 ± 0.0002	1.150 ± 0.0002	85.844/17
CMS [40]	2760	Charged	0.0972 ± 0.0006	1.145 ± 0.0002	83.860/19	0.0856 ± 0.0005	1.126 ± 0.0003	84.026/19	0.136 ± 0.002	1.169 ± 0.0001	110.614/19
CMS [30]	7000	Charged	0.101 ± 0.0009	1.152 ± 0.0004	64.009/24	0.0879 ± 0.0005	1.132 ± 0.0001	63.955/24	0.147 ± 0.001	1.179 ± 0.0002	80.316/24

Table 2: The fitting parameters T_4 and q_4 in (10), T_5 and n in (2), the errors of parameters, and χ^2/ndf for the particle spectra in $p + p$ collisions. The unit of T is GeV.

Data source	$\sqrt{s}$ (GeV)	Particle	T_4	q_4	χ_4^2/ndf	T_5	n	χ_5^2/ndf
PHENIX [37]	62.4	π^0	0.130 ± 0.0003	1.072 ± 0.0001	1.340/11	0.139 ± 0.0003	13.729 ± 0.121	1.302/11
PHENIX [25]	62.4	π^+	0.121 ± 0.0007	1.081 ± 0.002	5.386/23	0.131 ± 0.0002	11.867 ± 0.017	4.779/23
		π^-	0.114 ± 0.0002	1.085 ± 0.0001	5.402/23	0.125 ± 0.0003	11.661 ± 0.349	5.194/23
		K^+	0.111 ± 0.0004	1.104 ± 0.004	5.423/13	0.160 ± 0.0004	9.384 ± 0.011	5.121/13
		K^-	0.119 ± 0.001	1.089 ± 0.0001	2.271/13	0.161 ± 0.0001	10.95 ± 0.007	2.186/13
		p	0.099 ± 0.0002	1.071 ± 0.0003	7.861/24	0.176 ± 0.0001	16.099 ± 0.281	6.966/24
		$\overline{p}$	0.119 ± 0.0004	1.055 ± 0.0003	4.136/22	0.149 ± 0.0008	12.854 ± 0.005	7.178/22
PHENIX [38]	200	π^0	0.108 ± 0.0001	1.106 ± 0.0001	20.705/22	0.115 ± 0.0004	9.180 ± 0.018	23.025/22
PHENIX [25]	200	π^+	0.0971 ± 0.001	1.122 ± 0.002	4.740/24	0.115 ± 0.0008	8.291 ± 0.025	4.485/24
		π^-	0.107 ± 0.0002	1.113 ± 0.0006	3.352/24	0.122 ± 0.0001	8.848 ± 0.020	3.354/24
		K^+	0.0531 ± 0.0003	1.165 ± 0.009	1.665/13	0.136 ± 0.0009	6.222 ± 0.315	1.587/13
		K^-	0.0915 ± 0.0006	1.133 ± 0.009	4.321/13	0.148 ± 0.0009	6.941 ± 0.081	2.999/13
		p	0.0372 ± 0.0003	1.117 ± 0.002	22.734/31	0.142 ± 0.0002	8.164 ± 0.006	24.581/31
		$\overline{p}$	0.0481 ± 0.0001	1.109 ± 0.0001	15.932/31	0.151 ± 0.0009	9.210 ± 0.006	13.535/31
STAR [39]	200	π^+	0.113 ± 0.003	1.103 ± 0.002	5.743/20	0.127 ± 0.0001	9.725 ± 0.001	5.972/20
		π^-	0.115 ± 0.0002	1.101 ± 0.0001	5.144/20	0.129 ± 0.0002	9.912 ± 0.011	4.705/20
		p	0.0703 ± 0.0001	1.101 ± 0.0001	11.452/17	0.174 ± 0.0001	10.736 ± 0.089	10.359/17
		$\overline{p}$	0.0709 ± 0.0001	1.101 ± 0.0002	9.769/17	0.177 ± 0.0004	10.751 ± 0.006	9.991/17
ALICE [26]	900	π^0	0.107 ± 0.0004	1.133 ± 0.0006	7.687/10	0.137 ± 0.0002	7.947 ± 0.002	7.537/10
ALICE [27]	900	π^+	0.107 ± 0.0006	1.130 ± 0.0001	13.871/30	0.125 ± 0.0005	7.703 ± 0.058	13.460/30
		π^-	0.111 ± 0.0001	1.123 ± 0.0003	11.199/30	0.128 ± 0.002	8.090 ± 0.601	12.483/30
		K^+	0.0689 ± 0.0035	1.178 ± 0.002	14.271/24	0.159 ± 0.0001	5.733 ± 0.017	12.980/24
		K^-	0.0875 ± 0.0001	1.157 ± 0.0003	7.515/24	0.168 ± 0.0007	6.588 ± 0.022	6.609/24
		p	0.0407 ± 0.0001	1.145 ± 0.0002	15.148/21	0.195 ± 0.0006	8.537 ± 0.008	13.974/21
		$\overline{p}$	0.0404 ± 0.0001	1.147 ± 0.0002	15.637/21	0.190 ± 0.0008	8.660 ± 0.379	13.675/21
ALICE [41]	2760	π^0	0.123 ± 0.0002	1.137 ± 0.0002	5.979/15	0.142 ± 0.002	7.300 ± 0.112	5.987/15
ALICE [36]	2760	$\pi^+ + \pi^-$	0.110 ± 0.0002	1.142 ± 0.0003	30.885/60	0.130 ± 0.0002	7.034 ± 0.001	31.583/60
		$K^+ + K^-$	0.123 ± 0.0001	1.140 ± 0.0001	13.608/55	0.193 ± 0.0003	7.131 ± 0.0008	14.481/55
		$p + \overline{p}$	0.104 ± 0.0002	1.119 ± 0.0004	21.531/46	0.216 ± 0.0003	8.484 ± 0.0005	32.877/46
ALICE [26]	7000	π^0	0.120 ± 0.0005	1.145 ± 0.001	13.240/30	0.139 ± 0.0003	6.885 ± 0.006	16.750/30
ALICE [42]	7000	$\pi^+ + \pi^-$	0.105 ± 0.0002	1.160 ± 0.0004	26.539/38	0.128 ± 0.0004	6.257 ± 0.0002	26.216/38
		$K^+ + K^-$	0.131 ± 0.0002	1.154 ± 0.0003	5.373/45	0.206 ± 0.0003	6.497 ± 0.009	5.333/45
		$p + \overline{p}$	0.140 ± 0.0002	1.114 ± 0.0002	13.768/43	0.247 ± 0.0006	8.750 ± 0.006	12.700/43
CMS [30]	900	charged	0.115 ± 0.0001	1.129 ± 0.0005	85.776/17	0.126 ± 0.0002	7.627 ± 0.018	84.867/17
CMS [40]	2760	charged	0.117 ± 0.0004	1.144 ± 0.0001	110.770/19	0.137 ± 0.005	6.915 ± 0.035	110.4/19
CMS [30]	7000	charged	0.124 ± 0.004	1.152 ± 0.0001	80.353/24	0.145 ± 0.0003	6.583 ± 0.014	80.25/24

from ALICE Collaboration using the five distributions: (5) (solid line), (8) (dashed line), (9) (dotted line), (10) (dash-dotted line), and (2) (bold dash-dotted line), respectively. Since the lines are so close to each other, they are almost indistinguishable in the figures. To visualize the fitting quality better, we also plot the ratios of experimental data and fitting results at the bottom of the figures. We can see that the five distributions can describe the experimentally measured π^+ transverse momentum spectra very well. The errors are within 20%.

To show the fitting results other than pions, we select $K^+ + K^-$ at $\sqrt{s} = 2760$ GeV and $p + \overline{p}$ at $\sqrt{s} = 7000$ GeV at LHC in Figures 3 and 4, respectively. For the five distributions, we can not distinguish them at all in the two cases. Similar to pions, the fitting qualities are also very good.

As we can see from Tables 1 and 2, the values of parameter T_i are different. It is the main purpose of this work to target what causes the temperature discrepancies among different Tsallis distributions, with and without thermodynamical description. In order to avoid confusion, we emphasis the meaning of each T_i. Using the Tsallis distribution classification in [21], T_1 refers to Type B Tsallis distribution and T_5 refers to Type A Tsallis distribution. T_2, T_3, and T_4 are from the transient distributions to bridge Type A and Type B Tsallis

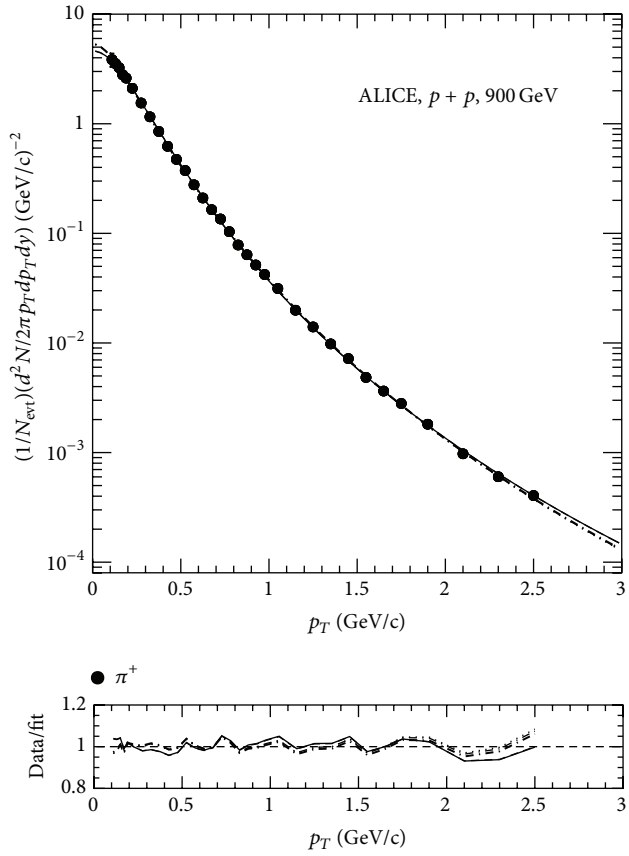

FIGURE 2: Same as in Figure 1 for π^+ in $p + p$ collisions at $\sqrt{s} = 900$ GeV. Data are taken from ALICE [27].

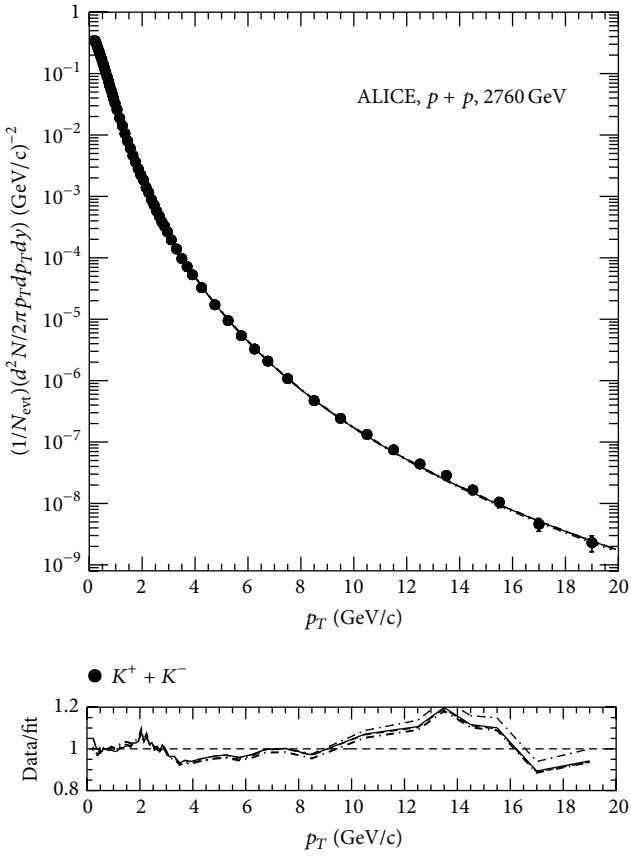

FIGURE 3: Same as in Figure 1 for $K^+ + K^-$ in $p + p$ collisions at $\sqrt{s} = 2760$ GeV. Data are taken from ALICE [36].

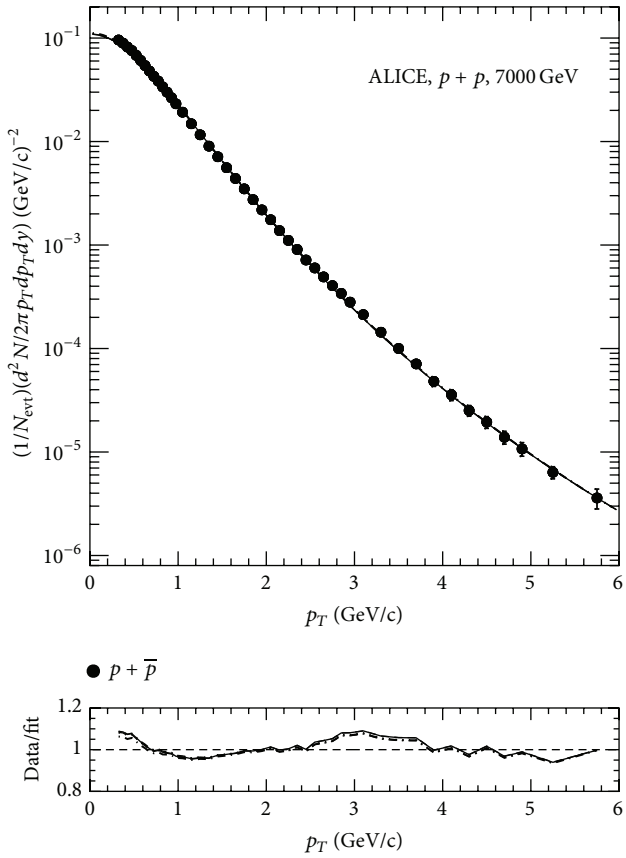

FIGURE 4: Same as in Figure 1 for $p + \overline{p}$ in $p + p$ collisions at $\sqrt{s} = 7000$ GeV. Data are taken from ALICE [42].

distributions. To have a clear picture for the parameter T_i from the five distributions, we plot T_i versus the colliding energy $\sqrt{s}$ for π, K, and p, as shown in Figure 5. We can clearly see that Type B Tsallis distribution gives lower T than Type A Tsallis distribution, as we mentioned in [21]. For the light particles, that is, pions (Figure 5(a)), T_1 and T_2 which are from the distributions ((5) and (8)) with extra m_T term are lower than T_3, T_4, and T_5 which are from the distributions ((9), (10), and (2)) without it. As we see that T_1 is larger than T_2, since (5) and (8) are similar except the power in the distributions, we conclude that the power q in (5) causes larger T. This can be verified by comparing T_3 with T_4. With the same argument, since T_4 is smaller than T_5, m_T in (10) causes smaller T. To see the effects of q and m_T in the distribution, we can compare T_3 with T_5, which are similar. The effects of the power q causing larger T and m_T causing smaller T cancel each other. For the heavier particles, that is, kaons and protons (Figures 5(b) and 5(c)), the effect of m_T in (9) wins and T_3 is smaller than T_5. We note that the effect of the extra m_T term is crucial for the temperature difference between Type A and Type B Tsallis distributions, especially for the light particles, while for the heavier particles, the effect of the choice of m_T or E_T in the Tsallis distribution becomes more important as we can see that T_5 is larger than the other T_i for kaons and protons in Figure 5.

4. Summary

In this paper, we have presented a detailed investigation of two types of Tsallis distribution, with and without the thermodynamical description, by the p_T spectra measured from STAR and PHENIX Collaborations at RHIC and ALICE and CMS Collaborations at LHC. The power q in the Tsallis distribution with thermodynamical description is responsible for the thermodynamical consistency. To show a clear and complete comparison, another three transient distributions to bridge the two types of Tsallis distribution are also given. Good agreements are obtained, but they give different temperatures. Agreed with our previous work [21], the Tsallis distribution with thermodynamical description gives lower T than the ones given by the distribution without it. The extra term m_T in the Tsallis distribution with thermodynamical description is responsible for the discrepancies of the temperatures. But for the heavier particles, the effect of the choice of m_T or E_T in the Tsallis distribution beats the effect of the extra term m_T. The data for $p + p$ collisions at 8 and 13 TeV are expected to provide further support for the conclusions presented here.

Competing Interests

The authors declare that they have no competing interests.

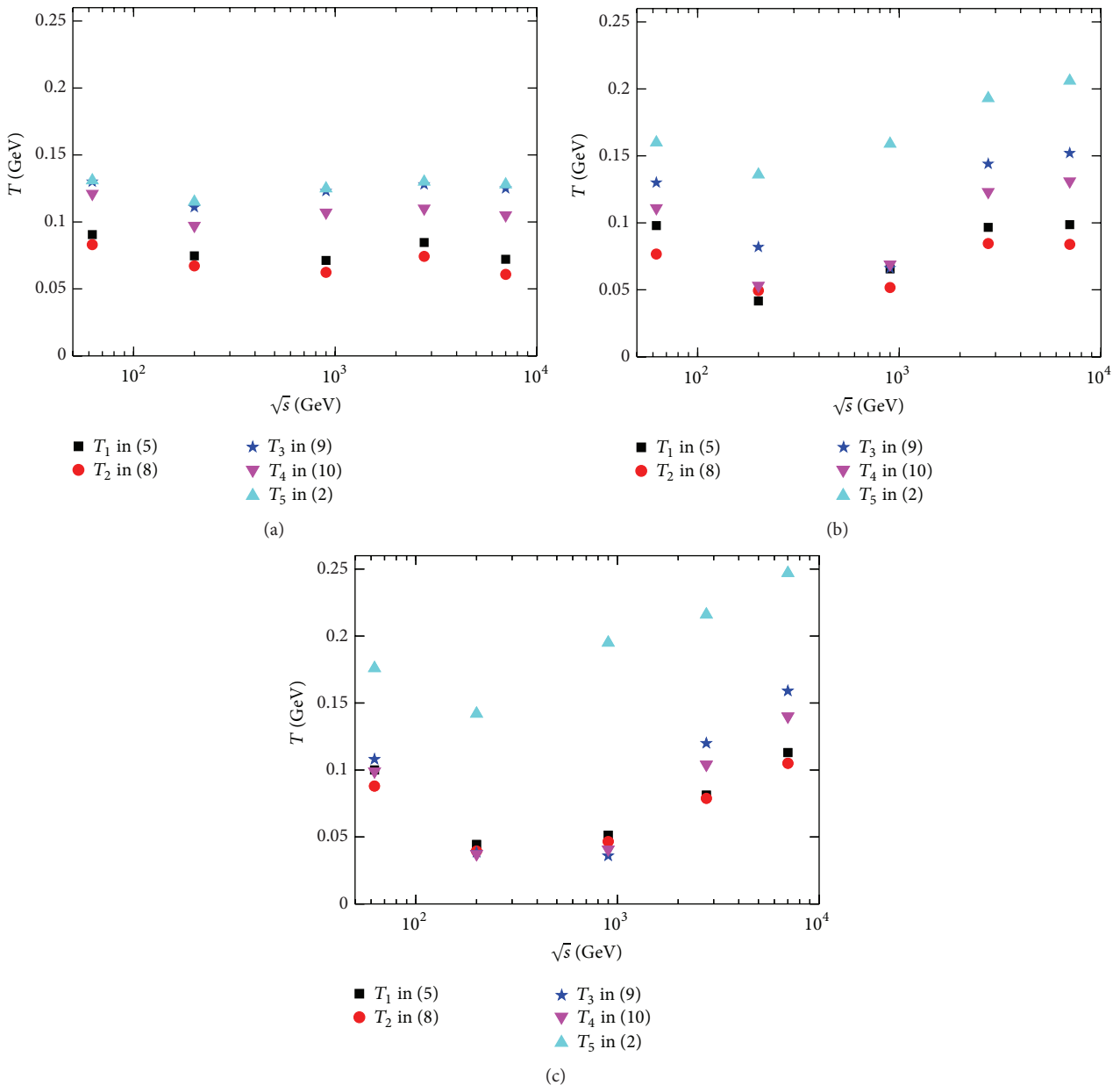

FIGURE 5: (Color online) temperature T in the five distributions versus $\sqrt{s}$ for (a) π, (b) K, and (c) p in $p + p$ collisions.

Acknowledgments

This work is supported by the NSFC of China under Grant no. 11205106.

References

[1] D. A. Teaney, "Viscous hydrodynamics and the quark gluon plasma," in *Quark-Gluon Plasma 4*, R. C. Hwa and X.-N. Wang, Eds., pp. 207–266, World Scientific, Singapore, 2010.

[2] M. Gyulassy and X.-N. Wang, "Multiple collisions and induced gluon bremsstrahlung in QCD," *Nuclear Physics B*, vol. 420, no. 3, pp. 583–614, 1994.

[3] R. C. Hwa and C. B. Yang, "Scaling behavior at high p_T and the p/π ratio," *Physical Review C*, vol. 67, Article ID 034902, 9 pages, 2003.

[4] V. Greco, C. M. Ko, and P. Lévai, "Parton coalescence and the antiproton/pion anomaly at RHIC," *Physical Review Letters*, vol. 90, no. 20, Article ID 202302, p. 4, 2003.

[5] I. Sena and A. Deppman, "Systematic analysis of p_T-distributions in p + p collisions," *The European Physical Journal A*, vol. 49, article 17, 5 pages, 2013.

[6] F.-H. Liu, Y.-Q. Gao, and B.-C. Li, "Comparing two-Boltzmann distribution and Tsallis statistics of particle transverse momentums in collisions at LHC energies," *The European Physical Journal A*, vol. 50, article 123, 11 pages, 2014.

[7] P. K. Khandai, P. Sett, P. Shukla, and V. Singh, "System size dependence of hadron p_T spectra in $p+p$ and Au+Au collisions

at $\sqrt{s_{NN}}$ = 200 GeV," *Journal of Physics G: Nuclear and Particle Physics*, vol. 41, no. 2, Article ID 025105, 10 pages, 2014.

[8] J. Cleymans and D. Worku, "The Tsallis distribution in proton–proton collisions at $\sqrt{s}$ = 0.9 TeV at the LHC," *Journal of Physics G: Nuclear and Particle Physics*, vol. 39, no. 2, Article ID 025006, 12 pages, 2012.

[9] M. D. Azmi and J. Cleymans, "Transverse momentum distributions in proton-proton collisions at LHC energies and Tsallis thermodynamics," *Journal of Physics G: Nuclear and Particle Physics*, vol. 41, no. 6, Article ID 065001, 10 pages, 2014.

[10] J. Cleymans, G. I. Lykasov, A. S. Parvan, A. S. Sorin, O. V. Teryaev, and D. Worku, "Systematic properties of the Tsallis distribution: energy dependence of parameters in high energy p-p collisions," *Physics Letters B*, vol. 723, no. 4-5, pp. 351–354, 2013.

[11] B.-C. Li, Y.-Z. Wang, and F.-H. Liu, "Formulation of transverse mass distributions in Au-Au collisions at $\sqrt{s_{NN}}$ = 200 GeV/nucleon," *Physics Letters B*, vol. 725, no. 4-5, pp. 352–356, 2013.

[12] M. Rybczyński and Z. Włodarczyk, "Tsallis statistics approach to the transverse momentum distributions in p-p collisions," *The European Physical Journal C*, vol. 74, article 2785, 5 pages, 2014.

[13] P. K. Khandai, P. Sett, P. Shukla, and V. Singh, "Hadron spectra in p+p collisions at RHIC and LHC energies," *International Journal of Modern Physics A*, vol. 28, no. 16, Article ID 1350066, 12 pages, 2013.

[14] C.-Y. Wong and G. Wilk, "Tsallis fits to p_T spectra and multiple hard scattering in pp collisions at the LHC," *Physical Review D*, vol. 87, no. 11, Article ID 114007, 19 pages, 2013.

[15] C.-Y. Wong and G. Wilk, "Tsallis fits to p_T spectra for pp collisions at the LHC," *Acta Physica Polonica B*, vol. 43, no. 11, pp. 2047–2054, 2012.

[16] C.-Y. Wong, G. Wilk, L. J. L. Cirto, and C. Tsallis, "From QCD-based hard-scattering to nonextensive statistical mechanical descriptions of transverse momentum spectra in high-energy pp and $p\overline{p}$ collisions," *Physical Review D*, vol. 91, no. 11, Article ID 114027, 16 pages, 2015.

[17] G. Wilk and Z. Włodarczyk, "Quasi-power laws in multiparticle production processes," *Chaos, Solitons & Fractals*, vol. 81, pp. 487–496, 2015.

[18] C. Beck, "Non-extensive statistical mechanics and particle spectra in elementary interactions," *Physica A*, vol. 286, no. 1, pp. 164–180, 2000.

[19] I. Bautista, C. Pajares, and J. Dias de Deus, "Evolution of particle density in high-energy pp collisions," *Nuclear Physics A*, vol. 882, pp. 44–48, 2012.

[20] L. L. Zhu, H. Zheng, and C. B. Yang, "Scaling behavior of transverse kinetic energy distributions in Au + Au collisions at $\sqrt{s_{NN}}$ = 200 GeV," *Nuclear Physics A*, vol. 802, no. 1–4, pp. 122–130, 2008.

[21] H. Zheng, L. Zhu, and A. Bonasera, "Systematic analysis of hadron spectra in p+p collisions using Tsallis distributions," *Physical Review D*, vol. 92, Article ID 074009, 7 pages, 2015.

[22] H. Zheng and L. Zhu, "Can tsallis distribution fit all the particle spectra produced at RHIC and LHC?" *Advances in High Energy Physics*, vol. 2015, Article ID 180491, 9 pages, 2015.

[23] C. Tsallis, "Possible generalization of Boltzmann-Gibbs statistics," *Journal of Statistical Physics*, vol. 52, no. 1-2, pp. 479–487, 1988.

[24] B. I. Abelev, J. Adams, M. M. Aggarwal et al., "Strange particle production in $p+p$ collisions at $\sqrt{s}$ = 200 GeV," *Physical Review C*, vol. 75, Article ID 064901, 21 pages, 2007.

[25] A. Adare, S. Afanasiev, C. Aidala et al., "Identified charged hadron production in $p+p$ collisions at $\sqrt{s}$ = 200 and 62.4 GeV," *Physical Review C*, vol. 83, no. 6, Article ID 064903, 29 pages, 2011.

[26] B. Abelev, A. Abrahantes Quintana, D. Adamová et al., "Neutral pion and η meson production in proton–proton collisions at $\sqrt{s}$ = 0.9 Tev and $\sqrt{s}$ = 7 Tev," *Physics Letters B*, vol. 717, no. 1–3, pp. 162–172, 2012.

[27] K. Aamodt, N. Abel, U. Abeysekara et al., "Production of pions, kaons and protons in pp collisions at $\sqrt{s}$ = 900 GeV with ALICE at the LHC," *The European Physical Journal C*, vol. 71, article 1655, 22 pages, 2011.

[28] B. Abelev, J. Adam, D. Adamová et al., "Multi-strange baryon production in pp collisions at $\sqrt{s}$ = 7 Tev with ALICE," *Physics Letters B*, vol. 712, no. 4-5, pp. 309–318, 2012.

[29] S. Chatrchyan, V. Khachatryan, A. M. Sirunyan et al., "Study of the inclusive production of charged pions, kaons, and protons in pp collisions at $\sqrt{s}$ = 0.9, 2.76, and 7 TeV," *The European Physical Journal C*, vol. 72, article 2164, 37 pages, 2012.

[30] S. Chatrchyan, V. Khachatryan, A. M. Sirunyan et al., "Charged particle transverse momentum spectra in pp collisions at $\sqrt{s}$ = 0.9 and 7 TeV," *Journal of High Energy Physics*, vol. 2011, no. 8, article 86, 38 pages, 2011.

[31] V. Khachatryan, A. M. Sirunyan, A. Tumasyan et al., "Transverse-momentum and pseudorapidity distributions of charged hadrons in pp collisions at $\sqrt{s}$ = 0.9 and 2.36 TeV," *Journal of High Energy Physics*, vol. 2010, article 41, 19 pages, 2010.

[32] V. Khachatryan, A. M. Sirunyan, A. Tumasyan et al., "Transverse-momentum and pseudorapidity distributions of charged hadrons in pp collisions at $\sqrt{s}$ = 7 Tev," *Physical Review Letters*, vol. 105, no. 2, Article ID 022002, 14 pages, 2010.

[33] S. Chatrchyan, V. Khachatryan, A. M. Sirunyan et al., "Study of the production of charged pions, kaons, and protons in pPb collisions at $\sqrt{s_{NN}}$ = 5.02 TeV," *The European Physical Journal C*, vol. 74, article 2847, 27 pages, 2014.

[34] J. Cleymans and M. D. Azmi, "Large transverse momenta and Tsallis thermodynamics," *Journal of Physics: Conference Series*, vol. 668, Article ID 012050, 4 pages, 2016.

[35] C. Y. Wong, *Introduction to High-Energy Heavy-Ion Collisions*, World Scientific, Singapore, 1994.

[36] B. Abelev, J. Adam, D. Adamová et al., "Production of charged pions, kaons and protons at large transverse momenta in pp and Pb-Pb collisions at $\sqrt{s_{NN}}$ = 2.76 Tev," *Physics Letters B*, vol. 736, pp. 196–207, 2014.

[37] A. Adare, S. Afanasiev, C. Aidala et al., "Inclusive cross section and double helicity asymmetry for π^0 production in $p + p$ collisions at $\sqrt{s}$ = 62.4 GeV," *Physical Review D*, vol. 79, Article ID 012003, 11 pages, 2009.

[38] A. Adare, S. Afanasiev, C. Aidala et al., "Inclusive cross section and double helicity asymmetry for π^0 production in $p + p$ collisions at $\sqrt{s}$ = 200 GeV: implications for the polarized gluon distribution in the proton," *Physical Review D*, vol. 76, Article ID 051106(R), 7 pages, 2007.

[39] J. Adams, M. M. Aggarwal, Z. Ahammed et al., "Identified hadron spectra at large transverse momentum in p+p and d+Au collisions at $\sqrt{s_{NN}}$ = 200 GeV," *Physics Letters B*, vol. 637, no. 3, pp. 161–169, 2006.

[40] S. Chatrchyan, V. Khachatryan, A. M. Sirunyan et al., "Study of high-p_T charged particle suppression in PbPb compared to pp collisions at $\sqrt{s_{NN}} = 2.76$ TeV," *The European Physical Journal C*, vol. 72, article 1945, 22 pages, 2012.

[41] B. Abelev, J. Adam, D. Adamová et al., "Neutral pion production at midrapidity in pp and Pb-Pb collisions at $\sqrt{s_{NN}} = 2.76$ TeV," *The European Physical Journal C*, vol. 74, article 3108, 20 pages, 2014.

[42] J. Adam, D. Adamová, M. M. Aggarwal et al., "Measurement of pion, kaon and proton production in proton-proton collisions at $\sqrt{s} = 7$ TeV," *The European Physical Journal C*, vol. 75, article 226, 23 pages, 2015.

[43] S. Chatrchyan, V. Khachatryan, A. M. Sirunyan et al., "Measurement of the Λ_b cross section and the $\overline{\Lambda}_b$ to Λ_b ratio with $J/\psi\Lambda$ decays in pp collisions at $\sqrt{s} = 7$ TeV," *Physics Letters B*, vol. 714, no. 2–5, pp. 136–157, 2012.

[44] B. I. Abelev, M. M. Aggarwal, Z. Ahammed et al., "Inclusive π^0, η, and direct photon production at high transverse momentum in $p + p$ and d + Au collisions at $\sqrt{s_{NN}} = 200$ GeV," *Physical Review C*, vol. 81, no. 6, Article ID 064904, 26 pages, 2010.

[45] W. M. Alberico and A. Lavagno, "Non-extensive statistical effects in high-energy collisions," *The European Physical Journal A*, vol. 40, no. 3, pp. 313–323, 2009.